JOURNAL OF MATERIALS SCIENCE 27 (1992) 2613–2618

Electroforming in MIM structure of SiO_x and SiO_x/SnO composite dielectric thin films

G. A. KHAN, C. A. HOGARTH
Department of Physics, Brunel University, Uxbridge, Middlesex UB8 3PH, UK

Electroforming and related phenomena in SiO_x and SiO_x–SnO thin films incorporated in copper–oxide–copper metal–insulator–metal structures have been investigated. Both types of devices showed voltage-controlled negative resistance, voltage memory effects (thermal and threshold) and electron emission. The voltage-controlled negative resistance and voltage memory effects may be interpreted in terms of the filamentary model of Dearnaley *et al.* The electron emission phenomenon is attributed to the Dearnaley model as modified by Rakhshani *et al.* The a.c. conductance of the devices before and after forming was also studied and the results support the proposed filamentary model of the electroforming process.

1. Introduction

In semiconductor device technology, the major use of oxides is as insulator or capacitor materials. The electrical conduction process in metal–insulator–metal (MIM) structures of thin (10–600 nm) insulating films at high applied fields obeys a general relationship of the type

$$I \propto \exp(\beta V^{1/2}/kT)$$

provided the applied voltage $V < V_F$, where V_F is the critical value of the applied voltage known as the forming voltage. However, if a sufficiently high applied voltage, commonly known as the threshold voltage $V_t \geqslant V_F$ is applied for a certain period of time (the forming time), such an insulating structure will acquire a permanently, irreversibly, enhanced conductivity. This novel growth of electrical conductivity is associated with the forming process and the device takes on its formed state. The process is distinctly different from dielectric breakdown which occurs at relatively higher electric fields and generally destroys the film itself [1, 2]. After forming, the MIM thin-film structure exhibits a voltage-controlled negative resistance (VCNR), electron emission into a vacuum, memory effects and switching. The VCNR and other related phenomena of formed devices have been explained using different theoretical approaches. Hickmott [3] and Simmons and Verderber [4] proposed that VCNR arises from a bulk property of an insulator. They have attempted to explain all the observed phenomena on a purely electronic basis. Greene *et al.* [5] suggested the forming process to be an unbalanced, high-field, solid-state electrolysis in the insulator in localized regions.

Knowing that the breakdown and partial breakdown processes in high-resistance materials are usually associated with the localized conduction paths where the current density is high, Dearnaley *et al.* [6] proposed a theory whereby the metal introduced during the forming process formed a series of metallic chains interspersed to some extent by vacancies. Such chains could be regarded as filamentary or poly-filamentary and various experiments involving microscopy and other less direct techniques have demonstrated beyond reasonable doubt the presence and importance of these filamentary paths in formed metal–oxide–metal structures. The VCNR is a result of the thermal rupture of such filaments. This theory was further revised by Sutherland [7]. The electroforming phenomena have been observed in many MIM structures. Apart from the early studies on SiO and Al_2O_3, such materials as Ta_2O_5, TiO, Nb_2O_5 and some sulphides have also been studied [4, 8–10].

A co-evaporation technique developed by Hogarth and Wright [11] has added a new dimension in this field of research. The object of this technique was to produce a better dielectric material as compared to the individual oxides. The authors were able to show that some of the dangling bonds in SiO thin films were satisfied by boron atoms and a mixed 70% SiO–30% B_2O_3 film showed much better dielectric properties as compared with those of simple SiO films. The electroforming behaviour of many oxide systems has been investigated in this laboratory [12–16]. Rahman *et al.* [17] studied the a.c. electrical properties of vacuum co-evaporated SiO–SnO_2 thin films. We have reported the d.c. properties of SiO_x–SnO composite thin films before forming elsewhere, and have proposed the Poole–Frenkel effect as being dominant at high electric fields. In this paper we present our studies of electroforming and other related phenomena in SiO_x and SiO_x–SnO thin layers.

2. Experimental procedure

The samples for electrical measurements were deposited on to 3 in. × 1 in. (76 mm × 25 mm) Corning 7059 borosilicate glass slides. In order to prepare MIM sandwiches, a metal strip was evaporated as the base electrode followed by mixed oxides from separate

0022–2461

sources as insulator using the co-evaporation technique of Hogarth and Wright [11], and finally evaporating metal via masks for the top electrodes. The rates of evaporation and film thickness could be controlled. Six devices, each having an effective area 0.1 cm^2, were made on each substrate.

All electrical measurements were taken in a subsidiary vacuum system at a pressure of about 10^{-5} torr (1.33×10^{-3} Pa) and equipped with the necessary facilities. The electrical connections to the devices were made by means of copper strips and joined with silver paste. A stainless steel tank incorporated into the top plate was used for low-temperature measurements by pouring liquid nitrogen into it. An insulated resistive wire made of molybdenum ribbon was inserted in the holes at the copper base and used as a heater element. The temperature measurements were made by attaching a Chromel–Alumel thermocouple to the substrate which was connected to a Comark electronic thermometer type 1601 Cr/A. The d.c. voltage–current characteristics were measured in a conventional manner. The bias voltage was supplied by a Coutant type LA100.2 power supply, and the circulating current was recorded by a Keithley 610C solid-state electrometer. The voltage across the sample was measured by a Farnell digital multimeter model DM131. The electrons emitted were attracted to a copper plate of size 2.5 cm × 7.6 cm × 0.25 cm placed just above the anode. The potential of the plate was kept at zero but care was taken to keep the distance between the anode and plate as small as possible (0.5 cm) to collect the maximum number of emitted electrons. The emission current was measured by a Keithley 610C solid-state electrometer.

3. Results

3.1. SiO_x thin films

The current–voltage characteristics of simple SiO_x (100 nm) thin films during the electroforming process are shown in Fig. 1. For the initial (first) cycle the circulating current up to an applied voltage of 4 V showed the well-known high-field behaviour related to the Schottky or the Poole–Frenkel effect (part a of the curve), which we have already discussed elsewhere. At the applied voltage of 4 V the circulating current became a function of time and started increasing continuously but slowly. The device was maintained at a fixed applied voltage of 4 V for a time period of 2 h until the current reached its saturated value. The rise in the circulating current under these conditions was about two orders of magnitude as can be seen in Fig. 1 (part b of the curve). The applied voltage was then increased beyond 4 V and the circulating current initially increased by a small value and then it started decreasing with the applied voltage, showing VCNR as shown by part c of the curve in Fig. 1. On the onset of VCNR, an emission current (part f of the curve) was also set up which increased very sharply with the increase in the applied voltage in the VCNR region. After the application of a maximum voltage of about 30 V, the applied voltage was decreased slowly and the circulating current followed the path as shown by

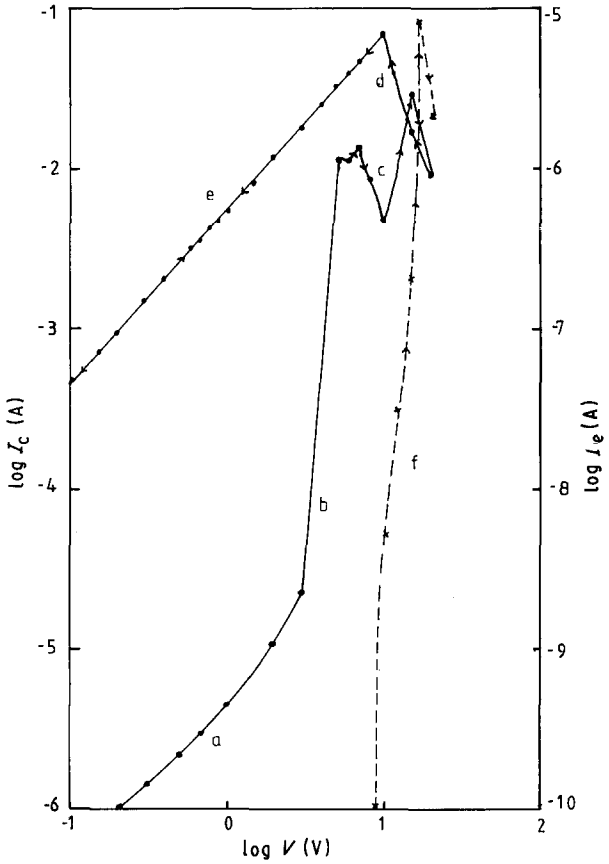

Figure 1 $I(V)$ plots for SiO_x (100 nm) thin films in Cu–SiO_x–Cu structure showing electroforming, VCNR and emission current.

curve d in Fig. 1. The circulating current increased initially on reducing the applied voltage until it attained its maximum value at a voltage of about 5 V. After that the circulating current decreased in a manner in which the current is directly proportional to the applied voltage as indicated by part e of the curve in Fig. 1. Part e of the $I(V)$ characteristics was found to be reproducible provided that the maximum applied voltage did not exceed the threshold voltage V_t.

The voltage memory effect in SiO_x (100 nm) thin films is shown in Fig. 2. The applied voltage was increased up to 25 V and a VCNR region was achieved. Then the applied voltage was suddenly switched off and the $I(V)$ characteristics of the device were again measured, showing a threshold voltage memory effect as shown in Fig. 2 (part b of the curve). In order to study the thermal voltage memory effect, the $I(V)$ characteristics of the formed SiO_x device were initially measured at room temperature for both forward and reverse cycles as shown in Fig. 3. The temperature of the formed device was then lowered to 153 K and the $I(V)$ characteristics were measured again. The first forward cycle showed a VCNR with a small increase in the value of I_m (the maximum value of the circulating current) which is represented by the dashed curve a in Fig. 3. On reducing the applied voltage the $I(V)$ characteristics followed the path as shown by the dashed line b in Fig. 3. For all other cycles the $I(V)$ characteristics followed the same pattern as that of line b, and no VCNR was achieved provided the temperature of the device remained low. At room temperature the VCNR was again observable on the

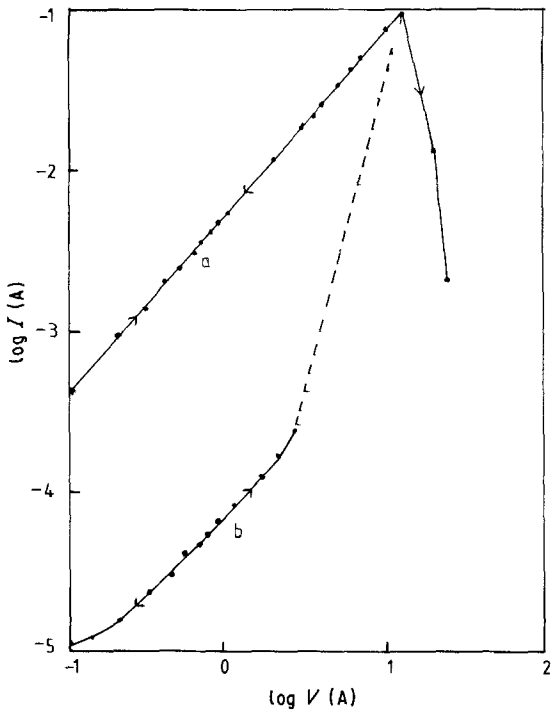

Figure 2 Threshold-voltage memory effect shown by the sample as in Fig. 1.

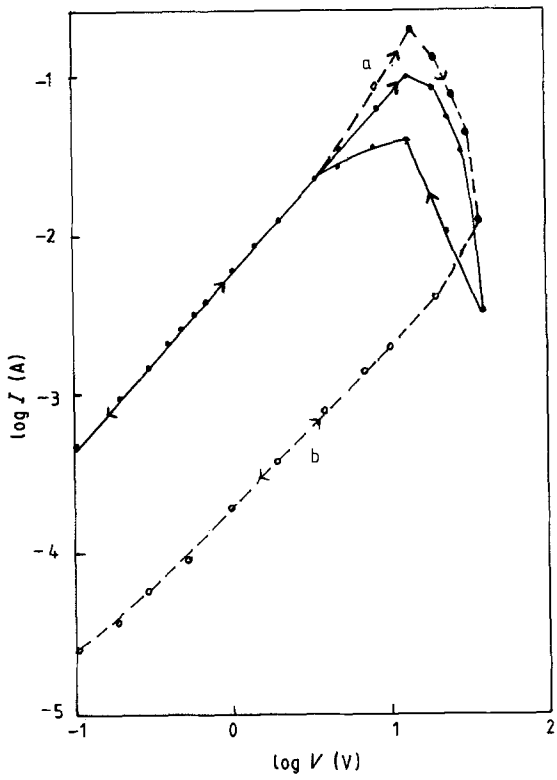

Figure 3 Thermal-voltage memory effect shown by the sample as in Fig. 1.

application of a voltage in excess of V_t. The a.c. conductance of the device both before and after electroforming can be seen in Fig. 4. The pressure–voltage memory effect could not be observed in our samples. Fig. 5 shows a scanning electron micrograph of the top electrode after the emission current was observed in SiO_x (100 nm) thin films.

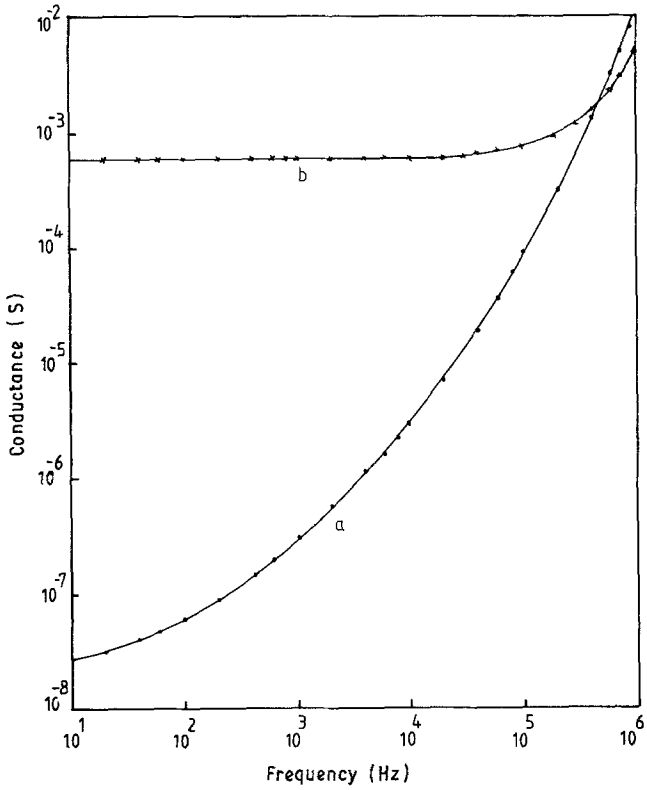

Figure 4 A.c. conductance versus frequency for the same sample as in Fig. 1, (a) before electroforming and (b) after electroforming.

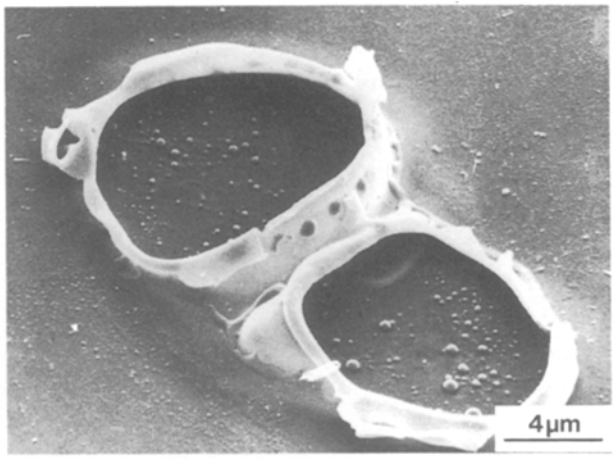

Figure 5 Scanning electron micrograph of top electrode of the sample as in Fig. 1 after electron emission.

3.2. SiO_x/SnO thin films

The measurement process for Cu–SiO_x/SnO–Cu devices was similar to that for Cu–SiO_x–Cu devices. Fig. 6 shows the electroforming VCNR and emission current in 90% SiO_x/10% SnO (100 nm) thin films. Threshold voltage and thermal voltage memory effects can be seen in Figs 7 and 8, respectively. The a.c. conductance both before and after electroforming is shown in Fig. 9. A scanning electron micrograph of the top electrode of a 90% SiO_x/10% SnO (100 nm) sample after electron emission may be seen in Fig. 10.

4. Discussion

The electroforming process in our devices (Fig. 1) can be related to the growth of conducting filaments as

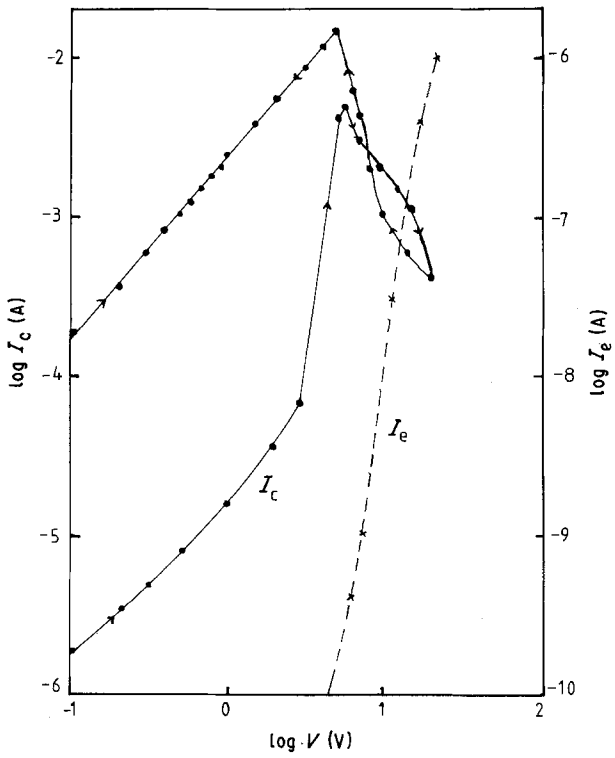

Figure 6 $I(V)$ plots for 90% SiO_x/10% SnO (100 nm) thin films in copper–oxide–copper structure showing electroforming, VCNR and emission current.

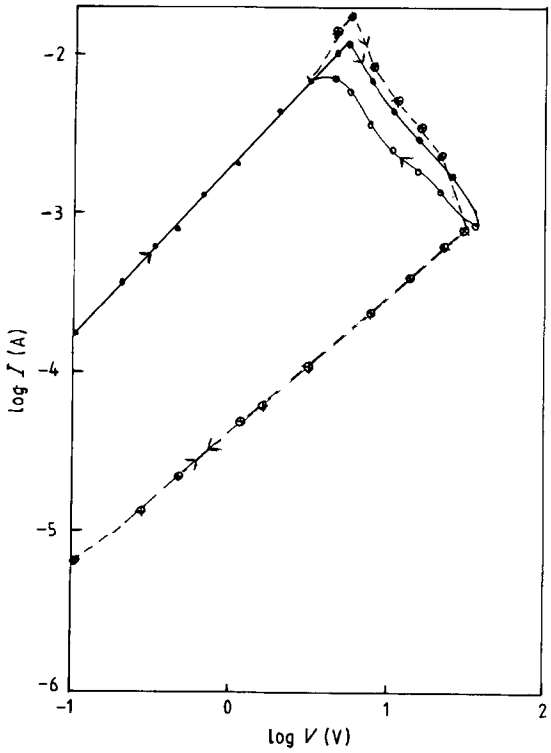

Figure 8 Thermal-voltage memory effect shown by the same sample as in Fig. 6.

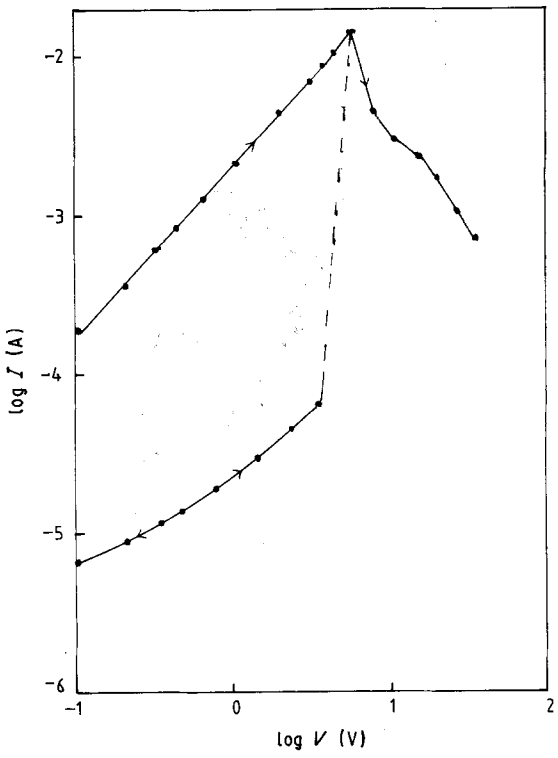

Figure 7 Threshold-voltage memory effect shown by the same sample as in Fig. 6.

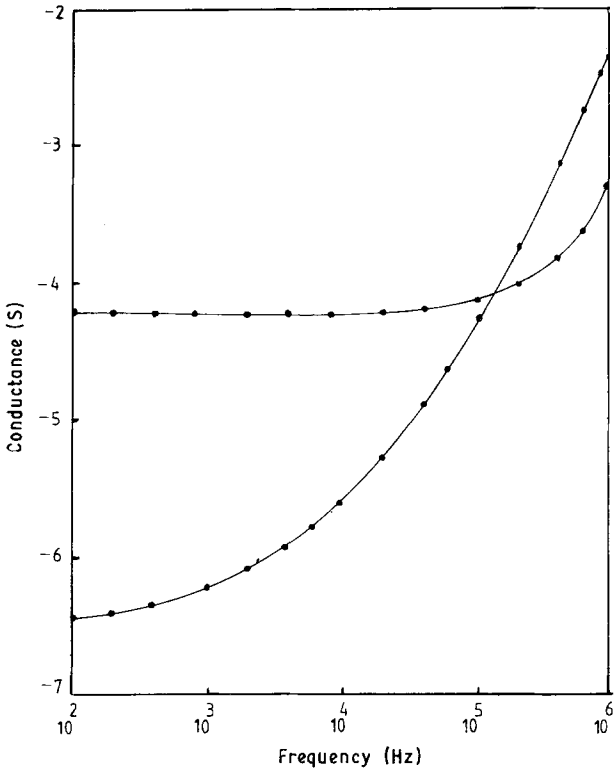

Figure 9 A.c. conductance versus frequency shown by the same sample as in Fig. 6, (a) before electroforming and (b) after electroforming.

suggested by Dearnaley *et al.* [6]. These conducting filaments bridge the gap between the cathode and anode and a high-conductivity state is induced in the devices. The distribution of these filaments may not be uniform and when significant power is being dissipated, as a result of the Joule heating effect, these filaments can rupture at their weak spots so that the conduction is reduced. The appearance of VCNR at higher voltages can be attributed to this type of rupturing of filamentary paths. The increase in the circulating current with the slow reduction of applied voltage during the reverse cycle can be related to a sort

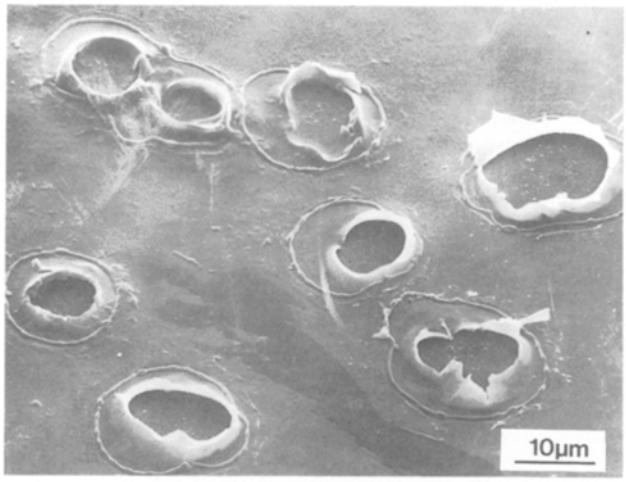

Figure 10 Scanning electron micrograph of top electrode of the same sample as in Fig. 6 after electron emission.

of temperature effect which can probably be explained in the following way. We suppose that after electroforming, the device has acquired a metallic character. With the decrease in the applied voltage in the negative resistance region of $I(V)$ characteristics, the Joule heating effect goes on decreasing. This will decrease the temperature of the device and also the resistance. This process will continue until the minimum value of device resistance is achieved and the Joule heating effect is reduced. Then the device will show a virtually metallic character as can be seen in part e of Fig. 1. This is consistent with the proposal of Dearnaley *et al.* [6] that the ruptured filaments can rejoin after a critical temperature. The constant behaviour of conductance with the frequency of a.c. field as shown in Fig. 9 can also be understood in terms of the highly conducting filaments which bridge the electrodes across the insulator.

The voltage memory effect is attributed to the fact that as the voltage is turned off suddenly when the device is in the state of negative resistance, the device will remain permanently in that particular state of filamentary condition because of the unavailability of the high voltage which is necessary for further rupturing or regrowth of filaments at that stage. For an applied voltage less than V_t the device will not change the high-impedance state at which it was turned off, because of the lower value of electric field which is less than that required for the start of filament regrowth. On the application of a voltage in excess of V_t, the regrowth of filaments will start and the device may regain its low-resistance state (erasing of voltage memory).

The appearance of VCNR during the first forward cycle which is related to the thermal-voltage memory effect can be explained in the following way. During the first cycle, because of some power dissipation a considerable amount of heat will be generated which will increase the device temperature, resulting in the rupture of filaments at weak spots. The hot electrons released from the broken filaments can scatter into the surrounding film matrix to polarize it. This will induce a high-resistance state of long relaxation time. On raising the device temperature, the device may be depolarized and rejoining of the filaments may occur on the application of a voltage in excess of V_t (erasing of thermal-voltage memory). A similar argument was put forward by Hogarth and Ilyas [18].

The electron emission process can be explained by the Dearnaley model as refined by Rakhshani *et al.* [19]. They suggested that the effective field across the device is not uniform and the regions of high field will lead to a solid-state electrolysis and to an excess of O^{2-} ions towards the anode and metal ions towards the cathode. We propose a general type of solid state electrolysis reaction as

$$2MO \rightarrow 2M^{2+} + 2O^{2-}$$

and

$$2O^{2-} \rightarrow O_2 + 4e^-$$

The electrons released in the above reaction may gain high energy near the anode and be emitted at the anode surface. At the low ambient pressure the oxygen gas so liberated may give rise to the peeling of the anode and hence the formation of holes on the electrode surface. This is very well confirmed by the scanning electron micrographs of our samples as in Fig. 10.

With the support of all the above observations we suggest the electroforming process in our devices to be governed by the filamentary model of Dearnaley *et al.* [6]. On the addition of SnO to SiO in SiO_x/SnO thin films, although the conductivity of the samples before forming is increased, the level of conduction (maximum current) after forming is somewhat less than that of pure SiO_x. This can be attributed to the dominance of the filaments of metallic carriers which find it harder to form by metallic diffusion in the SiO_x–SnO layers than in the simple SiO_x. Other behaviour related to the forming appears to be the same.

5. Conclusions

The electroforming process in both SiO_x and SiO_x/SnO thin-film sandwich structures and other effects such as VCNR and memory effects can be explained in terms of the filamentary model of Dearnaley *et al.* [6]. The a.c. behaviour of our samples before and after forming can be considered as a further confirmation of our suggestions. Electron emission into vacuum at the anode can be understood in terms of the Dearnaley model as modified by Rakhshani *et al.* [19].

References

1. T. W. HICKMOTT, *J. Appl. Phys.* **33** (1962) 2669.
2. A. K. RAY and C. A. HOGARTH, *Int. J. Electronics* **57** (1984) 1.
3. T. W. HICKMOTT, *J. Appl. Phys.* **35** (1964) 2679.
4. J. G. SIMMONS and R. R. VERDERBER, *Proc. R. Soc.* **A301** (1967) 77.
5. P. D. GREENE, E. L. BUSH and I. R. RAWLINGS, in "Thin Film Dielectrics", edited by F. Vratny (Electrochemical Society, New York, 1968) p. 167.
6. G. DEARNALEY, A. M. STONEHAM and D. V. MORGAN, *J. Non-Cryst. Solids* **4** (1970) 593.

7. R. R. SUTHERLAND, *J. Phys. D* **4** (1971) 468.
8. I. EMMER, *Thin Solid Films* **20** (1974) 43.
9. G. DOUCAS and D. WALSH, *ibid.* **9** (1971) 25.
10. K. L. CHOPRA, *J. Appl. Phys.* **36** (1965) 184.
11. C. A. HOGARTH and L. A. WRIGHT, in Proceedings of 9th International Conference on the Physics of Semiconductors, Moscow (Nauka, Leningrad, 1968) p. 1274.
12. M. ILYAS and C. A. HOGARTH, *J. Mater. Sci.* **18** (1983) 3377.
13. H. BIDADI and C. A. HOGARTH, *Thin Solid Films* **27** (1975) 319.
14. S.A. Y. AL-ISMAIL and C. A. HOGARTH, *J. Mater. Sci.* **20** (1985) 2186.
15. Z. T. AL-DHHAN and C. A. HOGARTH, *Phys. Status Solidi A* **110** (1988) 39.
16. W. I. KHLEIF, Z. T. AL-DHHAN and C. A. HOGARTH, *Int. J. Electronics* **65** (1988) 789.
17. A. S. MD. S. RAHMAN, M. H. ISLAM and C. A. HOGARTH, *ibid.* **62** (1987) 167.
18. C. A. HOGARTH and M. ILYAS, *Thin Solid Films* **103** (1983) 267.
19. A. E. RAKHSHANI, C. A. HOGARTH and A. A. ABIDI, *J. Non-Cryst. Solids* **20** (1976) 25.

Received 11 September
and accepted 26 September 1989